79-11-18
高工研図書室

DEUTSCHES ELEKTRONEN-SYNCHROTRON DESY

DESY 79/66
October 1979

# SPIN PARITY ANALYSIS OF THE DECAY $\tau \to \nu \rho \pi$

by

*PLUTO Collaboration*

NOTKESTRASSE 85 2 HAMBURG 52

To be sure that your preprints are promptly included in the
HIGH ENERGY PHYSICS INDEX ,
send them to the following address ( if possible by air mail ) :

DESY
Bibliothek
Notkestrasse 85
2 Hamburg 52
Germany

DESY 79/66
October 1979

# SPIN PARITY ANALYSIS OF THE DECAY $\tau \to \nu \rho \pi$

PLUTO Collaboration

W. Wagner[1]
I. Physikalisches Institut der RWTH Aachen

G. Alexander[2], L. Criegee, H.C. Dehne, R. Devenish[7], G. Flügge, J.D. Fox, G. Franke, Ch. Gerke, E. Hackmack, P. Harms, Th. Kahl[3], G. Knies, E. Lehmann, R. Schmitz, U. Timm, P. Waloschek, G.G. Winter, W. Zimmermann
Deutsches Elektronen-Synchrotron DESY, Hamburg

V. Blobel[4], A.F. Garfinkel[5], B. Koppitz, W. Lührsen
II. Institut für Experimentalphysik der Universität Hamburg

A. Bäcker, J. Bürger[1], K. Derikum, C. Grupen
Gesamthochschule Siegen

H. Meyer, M. Rössler, K. Wacker[6]
Gesamthochschule Wuppertal

(Submitted to Zeitschrift für Physik C)

Abstract

We have studied the $\tau \to \nu \rho^0 \pi$ decay in data taken with the PLUTO detector at the DORIS $e^+e^-$ storage ring, at CM energies from 4 to 5 GeV. We have found 27 events with the $\tau \to \nu \rho^0 \pi$ decay mode corresponding to a branching ratio of $B = (5.4 \pm 1.7)$ %. The Dalitz plot and the $\rho^0\pi$ mass spectrum are analysed for the $\rho\pi$ partial wave and spin state. Only the $\rho^0\pi$ s-wave as produced by the axial vector current gives a good description. The $\rho^0\pi$ mass spectrum is suggestive of an $A_1$ resonance. An upper limit on $\tau^\pm \to \nu \pi^\pm \pi^+ \pi^-$ without $\rho^0$ formation is given.

[1] Now at DESY, Hamburg, Germany.
[2] On leave from Tel-Aviv University, Ramat Aviv, Tel-Aviv, Israel.
[3] Now at MPI für Physik und Astrophysik, München, Germany.
[4] Now at CERN, Geneva, Switzerland.
[5] On leave from Purdue University, Lafayette, IN 47907, USA.
[6] Now at Harvard University, Cambridge, Mass., USA.
[7] Now at Oxford University, Oxford, U. K.



## I. Introduction

In a previous paper[1] (paper 1) we have reported evidence for the heavy lepton decay mode

$$\tau \to \nu \rho^0 \pi. \qquad (1)$$

The value observed for the branching ratio was in good agreement with the prediction[2] for a decay through the weak axial current into an $A_1$ meson, using Weinberg sum rules. This result supports the view of the $\tau$ as a sequential heavy lepton. On the other hand, the negative G-parity of the $\rho\pi$ final state alone is not sufficient to determine uniquely the current type of the decay interaction. The $\rho\pi$ final state also can originate from a second class vector current[3], or from a divergence of the axial current. In these cases it would carry spin parity quantum numbers of $J^P = 1^-$, or $J^P = 0^-$, respectively, rather than $J^P = 1^+$.

In this paper we report[4] on a spin parity analysis of the $\rho^0\pi$ final state in reaction (1), using the density distribution of the 3 pion Dalitz plot, and the shape of the $\rho^0\pi$ invariant mass distribution. The results confirm the $J^P = 1^+$ assignment and show that all other contributions are small.

Since in this analysis we use a larger sample of events for the decay (1) as in paper 1, we also give a new determination of the decay branching ratio.

## II. Experimental procedure

The decay (1) was observed in $\tau$ pair production events of the type:

$$e^+ e^- \to \tau + \bar{\tau} \to e^{\mp} (\mu^{\mp}) \nu\nu + \pi^{\pm} \pi^+ \pi^- \nu. \qquad (2)$$

The events were selected from data taken by the detector PLUTO at the storage ring DORIS at DESY, at CM energies W between 4 and 5 GeV.

Reaction (2) was found in 4 prong final states with an identified electron or muon. The electron identification[1,4] probability varied from 30 to 70 % for momenta from 400 to 1000 MeV/c and was constant for higher momenta. The probability for misidentifying a hadron track as electron was $(1.2 \pm .2)$ % for all momenta. Muons could be separated from hadrons at momenta $p > 1.0$ GeV/c, and the probability for misidentifying a hadron as muon was $(2.8 \pm .7)$ %[5]. The contamination by mistaking hadrons as leptons was determined from the corresponding 4 prong hadron event sample. To reduce this contamination it was useful to reject events

with a missing mass MM < 0.9 GeV/$c^2$. As discussed in paper 1, potential contributions from charmed meson decays are sufficiently suppressed by requesting the absence of photon conversions.

In total we find 69 events of the type $e^+e^- \to$ lepton ($\mu$,e) + 3 prongs,

with no associated $\gamma$ conversion,
and MM > 0.9 GeV/$c^2$. (3)

15 events of reaction (3) are kinematically not consistent with the $\tau$ pair production reaction (2), a number which matches the 11 events we expect from hadron-lepton misidentification for that kinematic configuration. There is no indication for lepton events in this category.

The other 54 events are kinematically consistent with reaction (2). For this kinematic configuration we expect a background of 18 events from hadron lepton misidentification. Thus there is a significant amount of lepton events. From the sample of lepton events with a visible $\gamma$ conversion we estimate a contribution of 6.5 events with associated but unconverted photons to sample (3). The remaining 29.5 events we attribute to the $\tau$ pair production reaction (2).

In the above check of the kinematic concistency, and in all further calculations we assume $\pi$ masses for the 3 non-lepton tracks.

## III. Decay mode and branching ratio

### III.1. The decay mode

In fig. 1 we show the distribution of the two $\pi^+\pi^-$ combinations per event, and of the higher mass combination (shaded histogram). We see a clear peak at the $\rho$ mass. The background distribution expected from hadron-lepton misidentification for the two combinations is indicated by circles. It shows no clear $\rho$ peak.

In this section we want to analyse which fraction of events contains a $\rho$ meson. For this purpose we have taken the observed $3\pi$ mass spectrum (fig. 2, histogram) and simulated its "decay" into 3 uncorrelated pions (3-body phase space) and into a $\rho^0\pi$ system. In table 1 we compare the number of events with at least one $2\pi$ mass combination in the $\rho^0$ band ($0.68 \le M_{2\pi} \le 0.86$ GeV/$c^2$) to those without any, for the data and the two simulated decay modes. We find that the observed events split in the same way as the simulated $\rho^0\pi$ decay mode, and that they split very differently from the direct $3\pi$ phase space decay. We conclude that our data agree with 100 % $\tau \to \nu\rho^0\pi$ decay. There is no indication for an uncorrelated $3\pi$ decay, and we



can infer an upper limit of

$$\frac{\Gamma(\tau^- \to \nu + (\pi^-\pi^+\pi^- \text{ uncorrelated}))}{\Gamma(\tau^- \to \nu + \rho^0\pi^-) + \Gamma(\tau^- \to \nu + (\pi^-\pi^+\pi^- \text{ uncorrelated}))} \le 0.20 \text{ at } 95\ \%\ \text{c.l.}$$

This result rules out the hypothesis[6] that the decay $\tau \to \nu\pi\pi\pi$ may be dominated by a contact term type diagram leading to 3 direct pions.

### III.2. Decay branching ratio $\tau \to \nu\rho\pi$

Since events with a $\pi\pi$ mass in the $\rho$ mass band ($0.68 < M_{2\pi} < 0.86$ GeV) have a considerably smaller background than the other ones (see table 1), we use only events from the $\rho$ mass band for the further analysis. Table 2 summarizes all numbers relevant for calculating the cross section of

$$e^+e^- \to \tau\tau \to (\mu,e)\,\nu\nu + \nu\rho^0\pi\,. \tag{4}$$

Assuming that electronic and muonic branching ratios are equal[5,7], we add the $e\rho^0\pi$ and $\mu\rho^0\pi$ events to determine the average for $B(\tau^-\to\nu\rho^0\pi^-)$. After subtracting the estimated contamination from hadron lepton misidentified events and from events with unconverted photons, and using the QED cross section for the production of pointlike $\tau$ pairs we find the product

$$B(\tau^+ \to \ell^+\nu\nu)\ B(\tau^- \to \nu\rho^0\pi^-) = 0.0093 \pm 0.0023. \tag{5}$$

In addition to the statistical error quoted above there is a systematic uncertainty of 16 % mainly from the efficiency correction of the event recognition (11 %) and the electron track reconstruction (9 %). Using a value of $B(\tau\to\ell\nu\nu) = 0.173 \pm 0.013$ [8] we arrive at $B(\tau\to\nu\rho^0\pi) = (0.054 \pm 0.013)\ (1.0 \pm 0.2)$ where the second factor gives the systematic error. Assuming $B(\tau\to\nu\rho^0\pi) = B(\tau\to\nu\rho\pi^0)$ we arrive at

$$B(\tau \to \nu\rho\pi) = (0.108 \pm 0.026)\cdot(1.0 \pm 0.2) \tag{6}$$

in good agreement with our previous result[1] of $(0.10 \pm 0.03)\cdot(1.0 \pm 0.2)$, and with the theoretical prediction of 0.081[2,8] for $\tau \to \nu A_1$.

## IV. Spin parity analysis of the Dalitz plot

In this section we want to investigate the spin parity quantum numbers of the $\rho\pi$ system. Some $J^P$ states can have 2 different $\rho\pi$ partial wave states. We therefore include the $\rho\pi$ orbital angular momentum value, $\ell$ in our notation.

Since the following analysis of the $\rho\pi$ system does not depend on the weak $\tau$ decay process, we consider also $J^P\ell$ states that cannot be produced through weak currents. We consider the following $J^P\ell$ quantum numbers: $0^-1$, $1^+0$, $1^+2$, $1^-1$, $2^-1$, and $2^+2$. For this low statistics analysis we do not consider mixtures of different $J^P\ell$ states.

The most significant consequences of the symmetries of the wave functions for the different $J^P\ell$ quantum numbers are zeros in the Dalitz plot density distribution. These zeros preferentially occur at the boundary and the center of the Dalitz plot. Let $T_i$ (i = 1,2,3) be the kinetic energies of the 3 pions in their CM system, and $\sum T_i = T_{tot} = M_{3\pi} - 3\, m_\pi$. Because the $M_{3\pi}$ values of our events have a broad distribution (see fig. 2) we use relative kinetic energies $T_i/T_{tot}$ in fig. 3 to achieve a representation of the Dalitz plot with practically the same boundary for all $M_{3\pi}$ values. In this representation the effect of the $\rho$-meson resonance and the cut for the $\rho$ band, however, is washed out.

For the further analysis we first consider the $\lambda$ projection[9] of the Dalitz plot to check qualitatively for the symmetry properties of the various $J^P\ell$ states. Secondly, we compare in a 3 dimensional Dalitz plot - with $M_{3\pi}$ as a third axis - the 3 dimensional density distributions of the various $J^P\ell$ states to the data to determine quantitative measures for their agreement.

IV.1. The $\lambda$ projection of the Dalitz plot

$\lambda$ is defined[9] by

$$\lambda = 1 - \frac{|\vec{p}_1 \times \vec{p}_2|^2}{3/4(1/9\, M_{3\pi}^2 - m_\pi^2)^2} \tag{7}$$

where $\vec{p}_1$, $\vec{p}_2$ are the momenta of $\pi_1$ and $\pi_2$ in the $3\pi$ cms. $\lambda$ measures at any value of $M_{3\pi}$, the relative (2 dimensional) distance of an event from the Dalitz plot center ($T_1 = T_2 = T_3$). $\lambda$ has the limits 0 (at the center) and 1 (at the boundary), for all values of $M_{3\pi}$.

Since the symmetry zeros in the density distribution preferentially occur at the boundary and the center of the Dalitz plot, the projection onto the distance variable $\lambda$ therefore should still exhibit the effect of these zeroes. In fig. 4 we compare the experimental $\lambda$ distribution to the expectations for the various $J^P\ell$ assignments under consideration. The full curve is the sum of the prediction



for 27 $\rho\pi$ events of the respective $J^P\ell$ state, added to the expectation for 13 background events (dashed curve). The predictions are calculated from the 3 dimensional distribution functions described in the next section. We see that for $J^P\ell = 1^+S$, $2^-P$ the agreement is good. In all other waves there are clear discrepancies at either $\lambda = 0$ (Dalitz plot center) or at $\lambda = 1$ (boundary), i.e. at points sensitive to the symmetries of the wave functions.

IV.2. Likelihood analysis in the 3 dimensional Dalitz plot

The density distribution in the Dalitz plot has the following form:

$$\begin{aligned} d^3N/dM_{3\pi}ds_1\, ds_2 &\equiv D(M_{3\pi},s_1,s_2;J,\ell) \\ &= A(M_{3\pi})\cdot H(s_1,s_2;J,\ell;M_{3\pi};m_\rho,\Gamma_\rho) \end{aligned} \tag{8}$$

with

$$\int ds_1\, ds_2\, H(s_1,s_2;J,\ell;M_{3\pi};m_\rho,\Gamma_\rho) = 1, \quad \text{for each } M_{3\pi} \text{ value,} \tag{9}$$

and

$m_\rho,\Gamma_\rho$ = mass and width of the $\rho$ meson.

$s_1 = (\pi_2 + \pi_3)^2$, and cyclic permutations.

$\pi_i$ is the four momentum vector of pion i. $s_1$ and $s_2$ are understood to be the masses of the neutral combinations.

The function H describes the density in the $s_1$ - $s_2$ plane; strictly speaking, there is a different density distribution for each $M_{3\pi}$ value. For H we use the approach of Frazer, Fulco and Halpern[10]. Here H accounts for (i) the symmetries of the respective $J^P\ell$ state wave functions, for effects from (ii) interference of 2 identical particles and (iii) from the $\rho$ resonance. Because of (9), the function A describes the $3\pi$ mass spectrum. It can be calculated in models of $\tau$ decay[11]. Since we here are interested in the symmetry properties only, we choose $A(M_{3\pi})$ to be equal to the experimental $3\pi$ mass spectrum of fig. 2 after background subtraction. Therefore, this analysis is independent of any assumption about the production process via a weak $\tau$ decay, and is also independent of the effect of $\rho\pi$ resonances on the $\rho\pi$ mass spectrum.

In the following we use (8) to compare the average likelihood of the data

$$L_{DATA}(J^P\ell) = \frac{1}{N}\sum_{events}^{N} \ell n D_i(M_{3\pi}, s_1, s_2; J, \ell), \qquad N = 40 \tag{10}$$

to the expectation

$$L_{MC+BG} = \frac{1}{N}\left\{ \underbrace{\sum_{i=1}^{N_{13}} \ell n D_i(\ldots; J, \ell)}_{\text{background}} + \underbrace{\sum_{j=N_{13}+1}^{N} \ell n D_j(\ldots; J, \ell)}_{\text{simulated } \rho\pi \text{ events}} \right\} \tag{11}$$

for the various $J^P\ell$ states. In (11) $N_{13}$ is a Poisson distributed number with $\langle N_{13}\rangle = 13$. In order to account for the cuts applied to the data, for each $J^P\ell$ state simulated $\rho\pi$ events were created according to (8) and the sum in (11) includes only events with these cuts. The contribution from the background events is determined from appropriate hadron + 3 prong events. Since there is a strong correlation between $M_{3\pi}$ and L, a simulation procedure was used that reproduced the experimental $M_{3\pi}$ distribution: In each mass bin of fig. 2, first the number of background events was chosen, Poisson distributed around the background expectation value, yielding $N_{13}$ events for the full mass spectrum. Then events from the respective $J^P\ell$ simulation were added to fill up the histogram bin by bin. In order to estimate the variance of $L_{MC+BG}$, in fig. 5 the L-distribution of 1000 of such samples of background and simulated events are plotted, for each partial wave. The value of $L_{DATA}$ is indicated by an arrow.

Only for two $J^P\ell$ values ($1^+0, 2^-1$) $L_{DATA}$ is reasonably well within the range of the expected distributions. In table 3 we summarize the probabilities, for the expected likelihood to be smaller than the observed one, for the various $J^P\ell$ values. This analysis of the likelihood in the 3 dimensional Dalitz plot confirms the observations in the projection onto the $\lambda$ variable.

## V. Partial wave analysis of the $\rho\pi$ mass spectrum

From the Dalitz plot analysis we found reasonable agreement with the data for $J^P\ell = 1^+0$ and $2^-1$. All other assignments were less probable by at least one order of magnitude. The $\rho\pi$ mass spectrum expected for the different $\ell$ values on the grounds of $\tau$ decay kinematics and angular momentum barrier factors[11] is shown in fig. 2. Only the s-wave resembles the experimental distribution ($\chi^2$ probability = 1 %) even though it does not reproduce the peak. However, with an



$A_1$ resonance (for parameters like $M \lesssim 1.2$ GeV and $0.4 < \Gamma < 0.5$ GeV) the peak can be well reproduced. In fig. 6 we show the curve for M = 1.0 GeV and $\Gamma = 0.475$ GeV ($\chi^2$ probability = 44 %).

The other $J^P\ell$ assignments lead to spectra shifted towards higher $\rho\pi$ masses, in clear disagreement with the data. No resonances are known in such partial waves which could bring them into agreement with the data. From fig. 2 we can estimate an upper limit for the fraction of events that could at most be attributed to a contribution from the second class vector current. We find zero events at $M_{3\pi} > 1.5$ GeV. This number is observed with 5 % probability for an expectation value of 3.0 events. Since 38 % of all events for $J^P\ell = 1^-1$ should have $M_{3\pi} > 1.5$ GeV, we have an upper limit of 7.9 events for vector current second class type events which corresponds to an upper limit of the branching ratio $B(\tau \to \nu\rho^0\pi,\ J^P = 1^-) < 1.6$ % at 95 % c.l.. The same numerical consideration applies to a pseudoscalar $\rho^0\pi$ state. If there is no interference, their sum is bounded by this upper limit value:

$$B(\tau \to \nu\, \rho^0\, \pi, \quad \text{with } J^P = 1^- \text{ or } 0^-) < 1.6\ \%.$$

## VI. Summary

In summary we find the decay $\tau \to \nu + 3\pi$ to be consistent with proceeding entirely through the chain $\tau \to \nu + \rho\,\pi \to \nu + 3\pi$, with a branching fraction of $B(\tau \to \nu\rho^0\pi) = 0.054 \pm 0.017$. The statistical error is 0.013, and there is a systematic normalisation uncertainty of 20 %. There is no evidence for a $3\pi$ decay without $\rho$ formation, and we find an upper limit (95 % c.l.) of $B(\tau^- \to \nu + \pi^-\pi^+\pi$, no $\rho^0) \leq 1.4$ %. The spin parity ($J^P$) of the $3\pi$ system was obtained from the symmetries of the Dalitz plot, assuming 100 % $\rho\pi$, and allowing for only one $\rho\pi$ partial wave state $\ell$ at a time. Under these assumptions only $J^P\ell$ values of $1^+0$ and $2^-1$ are acceptable.

The $\rho\pi$ mass distribution, however, excludes $J^P\ell = 2^-1$. The $J^P\ell = 1^+0$ state (axial current) gives a marginal description of the observed mass spectrum, but good agreement is achieved when an $A_1$ resonance is included in this partial wave. Also the $\rho^0\pi$ mass distribution imposes an upper limit (95 % c.l.) of 1.6 % to the branching fraction for the decay mode $\tau \to \nu\, \rho^0\, \pi$ with $J^P\ell = 1^-1$ (second class vector current) and $J^P\ell = 0^-1$ (divergence of the axial current).

Acknowledgements

We thank our technical staff for their indispensible contribution to the construction and operation of the PLUTO detector. We are indebted to the storage ring group for their excellent support during this experiment. We are also grateful to our cryogenic magnet group for their continuous services. We are very much indebted to Z. Rek and N. Kawamoto for help in the $\tau$-decay theoretical calculations. The non-DESY members of the PLUTO group would like to thank the DESY directorate for their kind hospitality. The work at Aachen, Hamburg and Siegen has been supported by the Bundesministerium für Forschung und Technologie.



References

1) PLUTO collaboration, G. Alexander et al., Phys. Lett. 73B (1978) 99.

2) Y.S. Tsai, Phys. Rev. D4 (1971) 2821;
H.B. Thacker and J.J. Sakurai, Phys. Lett. 36B (1971) 103.

3) S. Weinberg, Phys. Rev. 112 (1958) 1375.

4) See also: W. Wagner, Thesis, RWTH Aachen internal report PITHA 78/01 (unpublished).

5) PLUTO collaboration, J. Burmester et al., Phys. Lett. 68B (1977) 297;
Phys. Lett. 68B (1977) 301.

6) H. Goldberg, R. Aaron, Phys. Lett. 42 (1979) 339.

7) DASP Collaboration, R. Brandelik et al., Phys. Lett. 70B(1977) 125;
F.B. Heile et al., Nucl. Phys. B138 (1978) 189.

8) G.J. Feldman, SLAC-PUB-2230 (1978);
we use the average of $B_e$ and $B_\mu$.
G. Flügge, DESY report 79/37 (1979) and
Proc. of the Int. Conf. on High Energy Physics, Geneva, June 27 - July 4, 1979, to be published.

9) R.H. Dalitz, Phil. Mag. 44 (1953) 1068.

10) W.R. Frazer, J.R. Fulco and F.R. Halpern, Phys. Rev. 136B (1964) 1207.

11) N. Kawamoto, Z. Rek, private communication.

Table 1 Event numbers inside and outside the ρ mass band ($0.68 \leq M_{\pi^+\pi^-} \leq 0.86$ GeV), from events consistent with reaction (2)

| | Number of ρ combinations | |
|---|---|---|
| | ≥ 1 | 0 |
| Data | | |
| Total | 40 | 14 |
| Estimated background events from | | |
| misidentified leptons | 8.5 | 9.5 |
| unobserved photons | 4.5 | 2.0 |
| τ events | 27 ±6.5 | 2.5 ±4 |
| Decay simulation | | |
| ρπ decay | 23.6 | 5.9 |
| πππ decay | 12.7 | 16.8 |

Table 2 Numbers used for the determination of cross sections

| Luminosity ($nb^{-1}$) | 5050 | |
|---|---|---|
| Identified lepton events+ | e | μ |
| Total number of events | 34 | 6 |
| Estimated background events from | | |
| misidentified leptons | 6.5 | 2 |
| unobserved photons | 4.5 | < 0.5 |
| τ events | 23 | 4 |
| Detection probability++ | 0.054 ±0.009 | 0.034 ±0.004 |

+ ρ-sample: $0.68 \leq M_{\pi^+\pi^-} \leq 0.86$ GeV

++ Using V-A decay for the lepton momentum spectrum



Table 3 Probabilities for the various $J^P\ell$ assignments. The upper limits have a 95 % confidence level

| $J^P\ell$ | Probability from Dalitz plot density |
|---|---|
| $0^-1$ | < 0.3 % |
| $1^+0$ | 8.9 % |
| $1^+2$ | < 0.7 % |
| $1^-1$ | 0.6 % |
| $2^-1$ | 3.7 % |
| $2^+2$ | < 0.3 % |

Figure captions

Fig. 1 Distribution of the $\pi^+\pi^-$ masses (2 combinations per event). The shaded region gives the distribution for the higher mass, the circles represent the expected background from hadron-lepton misidentification (18 events).

Fig. 2 Invariant $\rho^0\pi$ mass distribution with a $\rho$ cut of $0.68 < M_{\pi^+\pi^-} < 0.86$ GeV/$c^2$. The curves are: the expected background (BG) for 13 events and, added to the background, the mass distribution calculated for an s, p and d wave for the $\rho\pi$ system in the $\tau \to \nu\,\rho\,\pi$ decay.

Fig. 3 Triangle Dalitz plot $T_1/T_{tot}$ vs. $|T_2 - T_3|/T_{tot}\,\sqrt{3}$ for the data (circles) compared to $J^P\ell = 1^+$ s-wave (points). $T_1$, $T_2$, $T_3$ are the kinetic energies of the $\pi^{\pm}$, $\pi^{\mp}$, $\pi^{\mp}$ in the $\pi\pi\pi$ rest frame, $T_{tot}$ is the total kinetic energy.

Fig. 4 Distribution of $\lambda$, the distance from Dalitz plot center, as defined in the text. Experimental events (histograms), expected background (dashed line), and the distribution of various spin-parity states (solid lines) added to the background.

Fig. 5 Distribution of 1000 average likelihood values from Monte-Carlo experiments for each of the different $J^P\ell$ assignments (including background). The values from the data are indicated by arrows.

Fig. 6 Invariant $\rho^0\pi$ mass distribution (as in fig. 2), compared to an s-wave without and with an imposed $A_1$ resonance of mass = 1.0 GeV/$c^2$ and width = 0.475 GeV/c (dashed curve), added to the expected background (solid curve) from hadron-lepton misidentification.

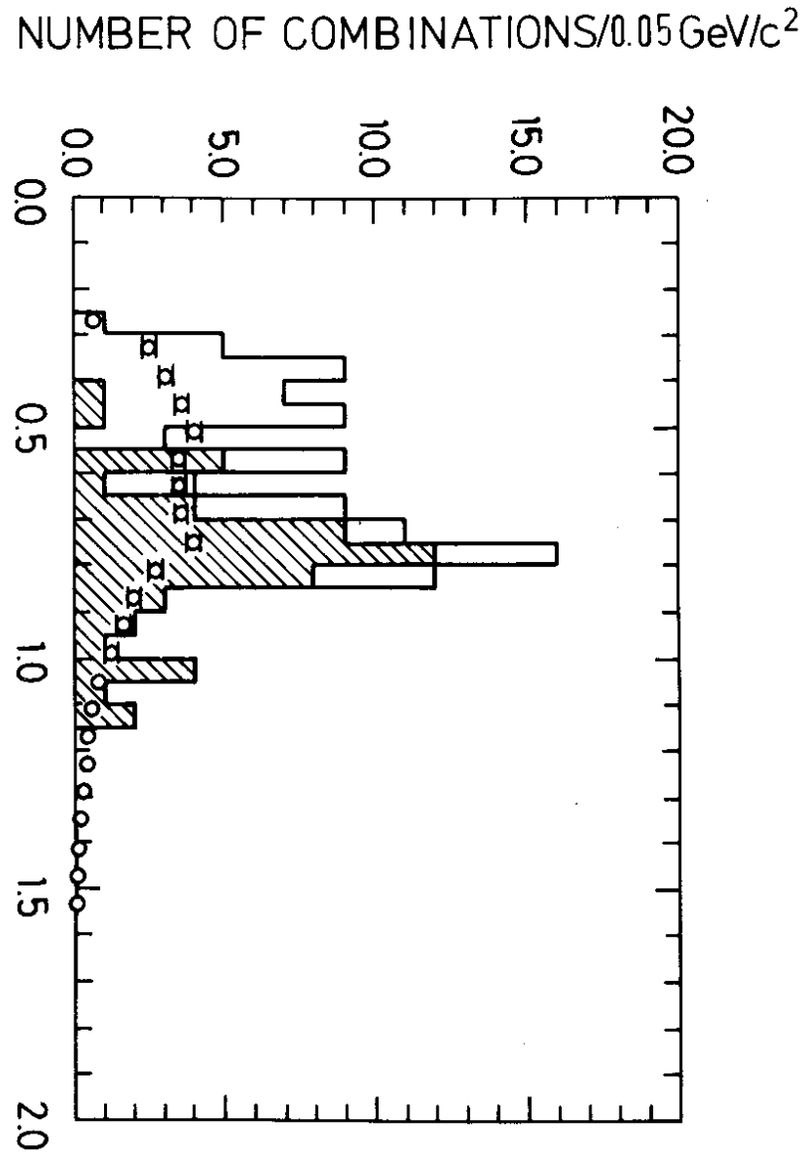


Fig. 1

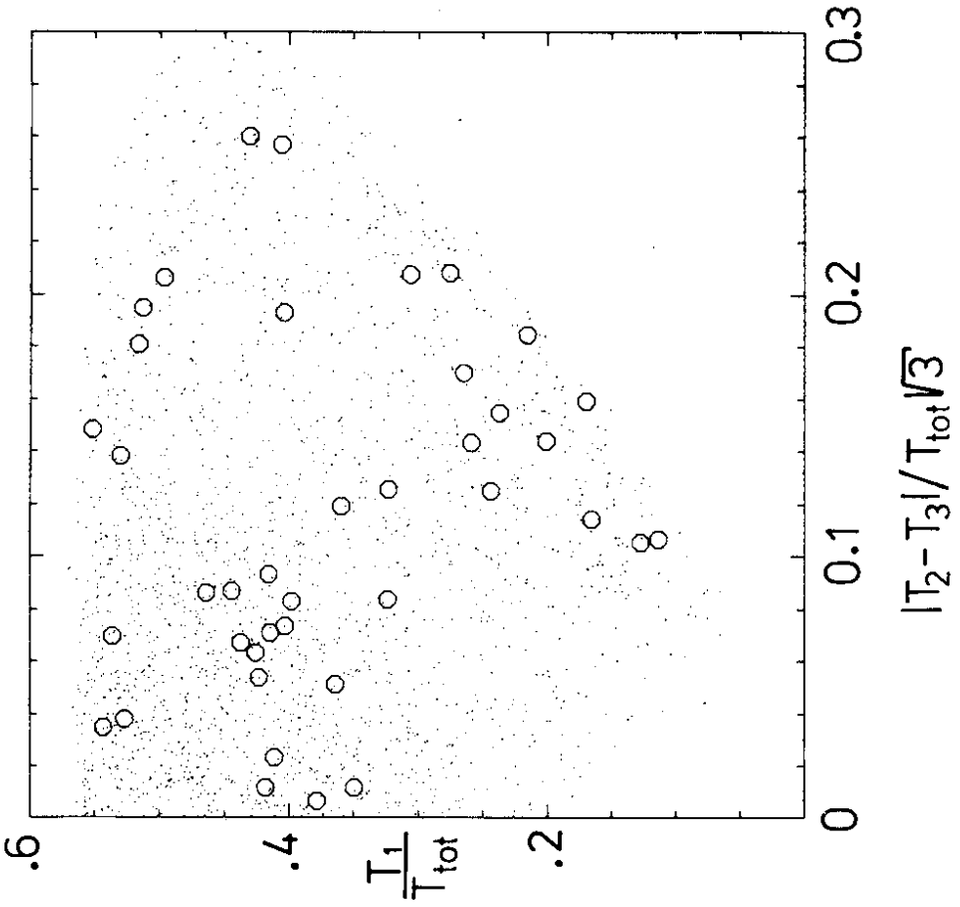
.6
.4
.2
0
0.1
0.2
0.3
$\frac{T_1}{T_{tot}}$
$|T_2 - T_3| / T_{tot}\sqrt{3}$

Fig. 3

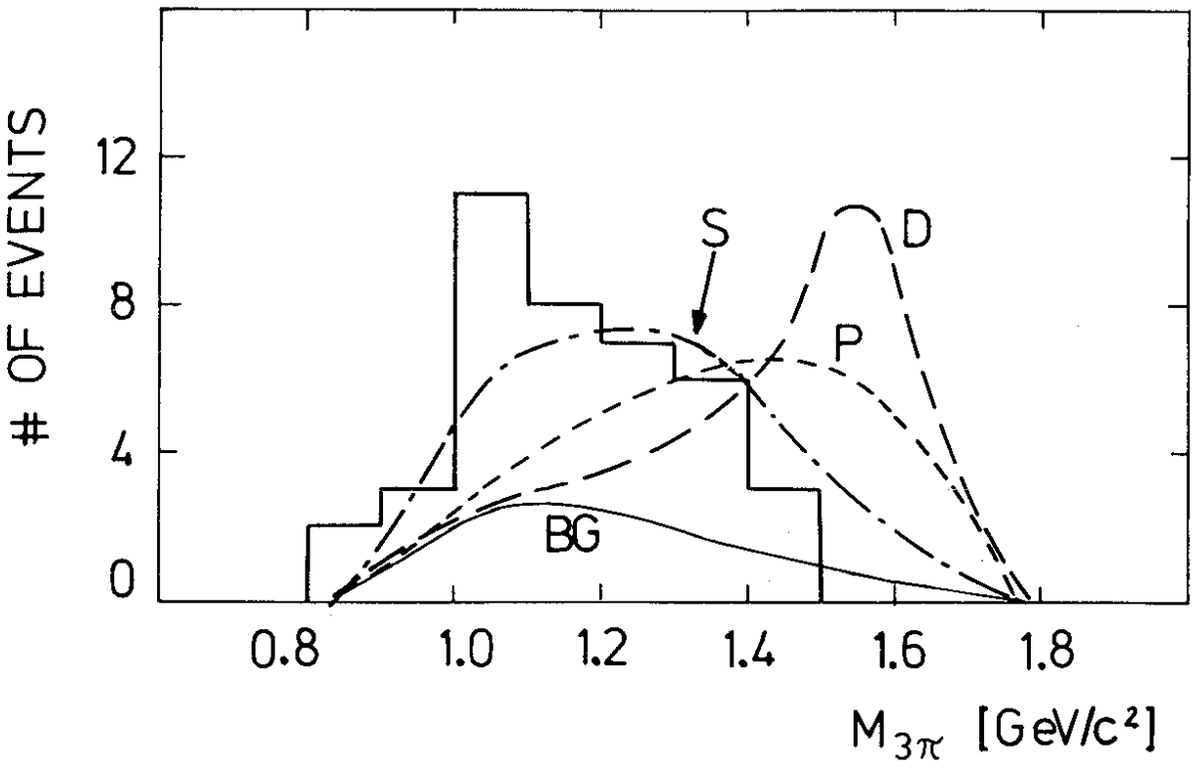
# OF EVENTS
0
4
8
12
S
D
P
BG
0.8
1.0
1.2
1.4
1.6
1.8
$M_{3\pi}$ [GeV/c²]

Fig. 2

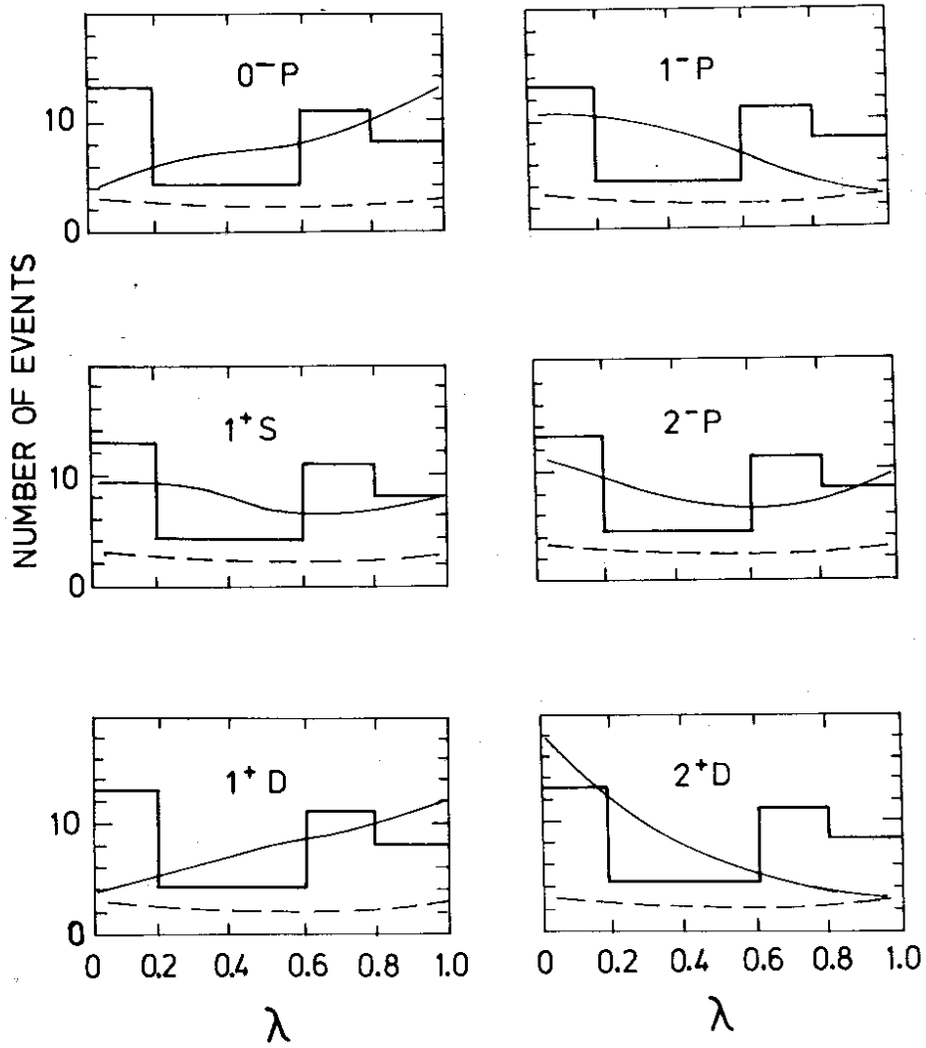
NUMBER OF EVENTS
0⁻P
1⁻P
1⁺S
2⁻P
1⁺D
2⁺D
10
0
0 0.2 0.4 0.6 0.8 1.0
λ

Fig. 4



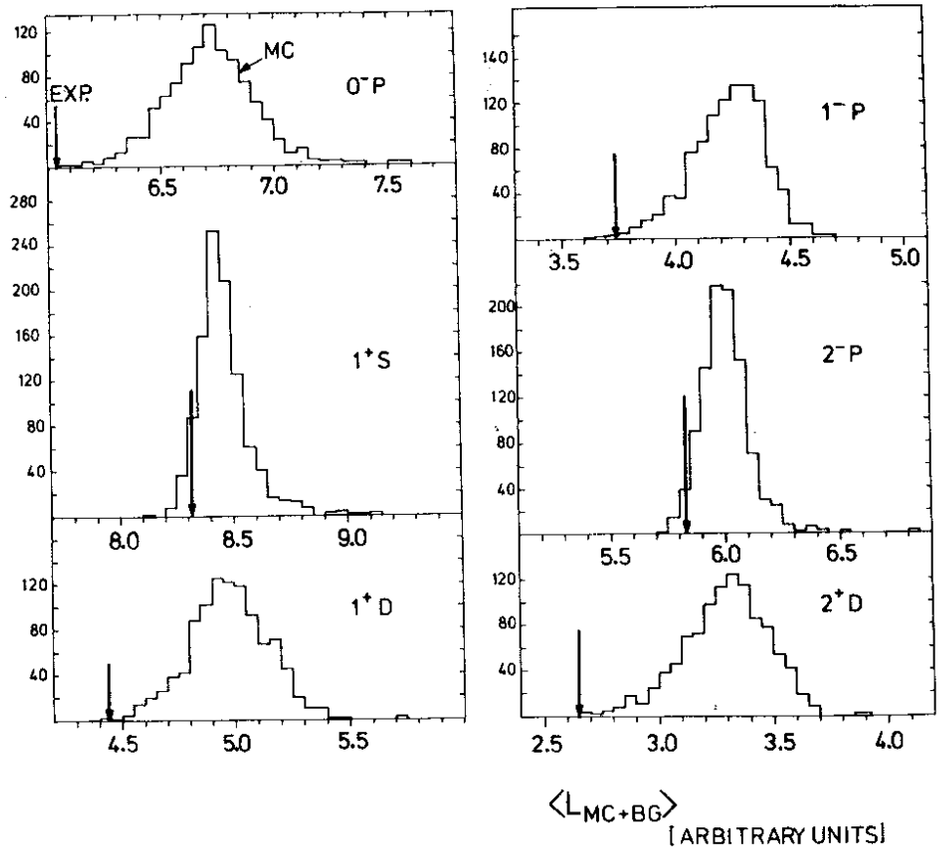
MC
EXP.
0⁻P
1⁻P
1⁺S
2⁻P
1⁺D
2⁺D
⟨L_MC+BG⟩
[ARBITRARY UNITS]

Fig. 5

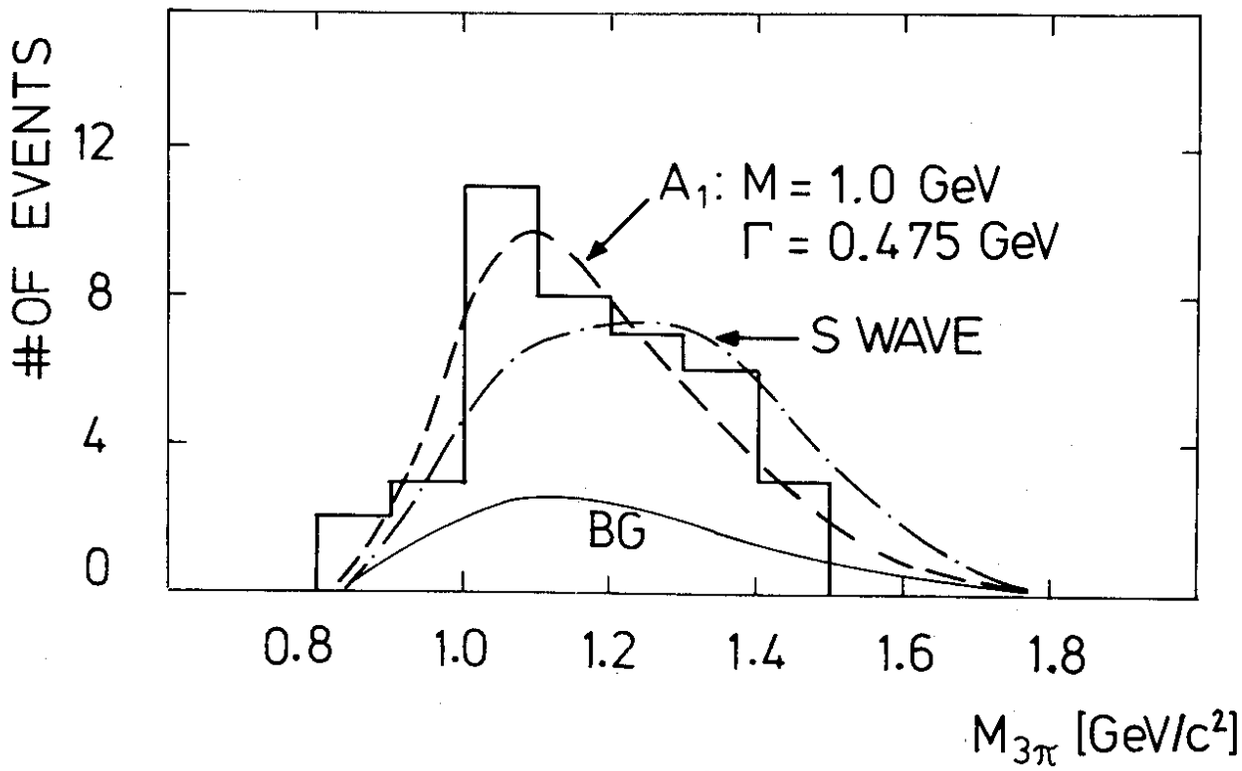
#OF EVENTS
12
8
4
0
A1: M = 1.0 GeV
Γ = 0.475 GeV
S WAVE
BG
0.8
1.0
1.2
1.4
1.6
1.8
M3π [GeV/c²]

Fig. 6